Journal of Applied Fluid Mechanics, Vol. 11, No. 4, pp. 957-963, 2018.
Available online at www.jafmonline.net, ISSN 1735-3572, EISSN 1735-3645.
DOI: 10.29252/jafm.11.04.28558

Preliminary Experimental Investigation on a Low Profile Magneto-Hydrodynamic Propulsive Blanket, Considering Plasma Generation

M. A. Feizi Chekab, P. Ghadimi†, M. Sheikholeslami and A. Ghadimi

Department of Marine Technology, Amirkabir University of Technology, Tehran, Iran

†*Corresponding Author Email: pghadimi@aut.ac.edu*

ABSTRACT

The use of magnetohydrodynamic (MHD) blanket propulsion system in ships, even with low efficiencies, has particular benefits that can make them an appropriate option for the marine designers. Accordingly, any attempt to increase the efficiency of these systems requires full recognition of their performance in different conditions. In the present study, as a continuation of previous numerical works by the current authors, a magneto-hydrodynamic blanket propulsion system has been built and experimentally studied through examining the MHD forces produced in different voltages. Copper and gold have been used and compared as electrodes and the high advantage of gold has been demonstrated. The effect of electrolysis on the behavior of the blanket is analyzed. It has been demonstrated that although electrolysis restricts high currents in lower voltages (lower than ~140V) and the saturation of hydrogen decreases the MHD forces due to low electrical current (~140V up to ~160V), the saturation of hydrogen around cathode at high voltages (more than ~160V), makes a dielectric barrier which soon breaks down and make the production of plasma possible, which in turn highly increases the thrust force of the MHD blanket. Therefore, three regimes have been introduced and described for the MHD blanket; the electrolysis regime, the transition regime, and the hot plasma regime. Based on the obtained results, one may conclude that the present results have offered good evidence about the possibility of increasing the MHD blanket performance through plasma production in water.

Keywords: MHD propulsive blanket; Electrolysis; Plasma; Experimental investigation

1. INTRODUCTION

In the maritime sector, the use of an optimal propulsion system for surface and submerged vehicles is always important, both in economic and design aspects. Conventional propulsion systems, despite their remarkable improvements, have many essential design constraints due to their mechanical moving parts. These limitations are barriers to innovative designs, which could be diminished by using propulsion systems with the least moving parts possible. Magneto-hydrodynamic (MHD) propulsion is one of these systems with no moving parts.

Although various researches have been conducted on the use of MHD propulsion system for ships, most studies still retain the same traditional mentality of thrust system, according to which the propulsion system should be concentrated in a certain region of the vehicle. In the following, a brief overview of the research conducted in this area is presented.

The MHD term seems to be firstly used by Alfven (1942). But earlier, Hartman and Lazarus (1937), are the first to study the theoretical and experimental aspects of magnetic flows in channels. Later, marine MHD propulsion systems were first presented by Rice (1961), Friauf (1961), and Way (1967) in their patents for MHD propulsion systems of surface and submarine vessels in the 60's. In the same context, the Yamato vessel was constructed as one of the most famous projects of MHD propulsion systems in the 1990s (Motora *et al.* 1991). The traditional approach to propulsion systems led the propulsion system of Yamato to be concentrated inside the hull and did not achieve significant success.

Despite the rather unsatisfactory results of the Yamato vessel, research on the MHD propulsion system continued to be conducted analytically, experimentally, and numerically. Numerical and experimental study of the effects of different electric and magnetic field strengths and patterns were conducted by Han *et al.* (2002) and by Lin *et al.* (1992), respectively. The effects of MHD channel shapes were evaluated numerically by Doss *et al.* (1990) and evaluated analytically and experimentally by Gilbert *et al.* (1995). Other research subjects in this field include the

improvement of water conductivity (Lin, 1990 and Lin *et al.* 1991), superconductors and cooling systems (Hales *et al.* 2006; Yan *et al.* 2002; Meng *et al.* 1991) and the stability of MHD systems (Abdollahzadeh, 2014). For a comprehensive overview of studies in this area, one may refer to the work of Weier *et al.* (2007).

Although the main focus of the present study is on the application of MHD in marine propulsion systems, the magneto-hydrodynamic interactions and forces is important in many other fields including aerospace, astrophysics (Stenflo 2015 and Skala *et al.* 2015), and metallurgy, and can play a decisive role in the field of modern technologies such as nanotechnology (Zhang et.al 2007) and fusion reactors (Dhanai et.al, 2015). Even in the field of fluid dynamics, in addition to the propulsion system, MHD is used in other areas including MHD generators and pumps (Smy, 1961; Kantrowitz, 1962) and flow control (Popov, 1971; Wu, 1973).

After introducing and optimizing the MHD propulsive blanket by the present authors (Feizi and Ghadimi 2016), the optimum design is experimentally tested in the present manuscript and the propulsion force and electrical behavior of the blankets are analyzed.

In the following section, the experimental setup is described. Afterward, the results are presented and analyzed.

2. EXPERIMENTAL SETUP

As described in an earlier work by Feizi and Ghadimi (2016), the MHD propulsive blanket is made of three layers:

a) Electrical layer which includes the electrodes for inducing the electrical current in the water.
b) Magnetic layer which includes the magnets for inducing the magnetic field.
c) Support layer which is made of a flexible material and provides the structural support.

In the present study, the blanket support layer has been built once by using 3D printer and once more by using a 3mm silicon sheet which are presented in Fig. 1.

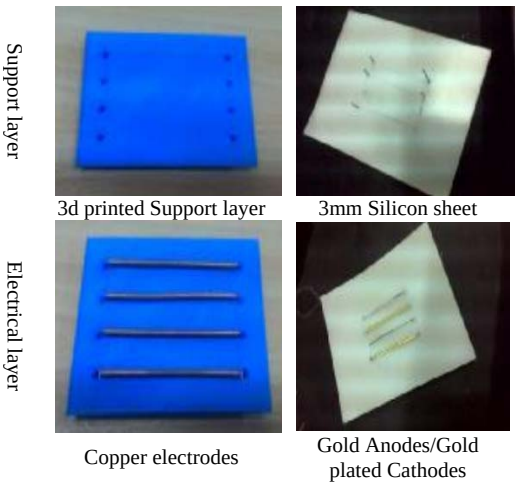

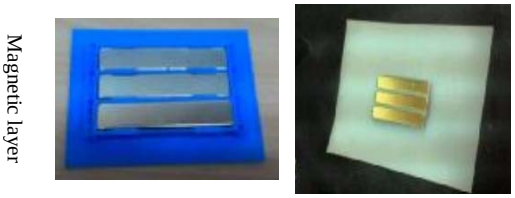

Fig. 1. MHD Blankets built and their different layers.

For the magnetic layer, three 50*10*3 mm Niobium magnets are used for both cases, which produce near 2300 G on each surface.

On the other hand, the electrical layer is made of copper electrodes for the printed case and Gold anodes and gold plated copper cathodes are used for the silicon one. The main reason for using the gold anodes is the appropriate resistance of gold against oxidization in anode, due to the electrolysis.

Since the blanket has to be tested under high voltages, anodes are required to be resistant to oxidization. For this purpose, before applying the electrodes to the blanket, two copper and gold electrodes are tested under different voltages and their oxidization behavior is examined. This test has a simple mechanism in which, using a variable voltage source, a variety of voltages are applied to the electrodes in a pond of salt water with 38 g/Liter salt.

When the electrolysis occurs, the oxidization in the anode causes a severe corrosion of the anode electrode. Since different materials have different oxidization behavior, in order to compare the oxidization of copper and gold in a separate experiment, the electrolysis was investigated separately with two samples of copper and gold electrodes placed under different voltages. Figure 2 displays the copper anode with a diameter of 3mm after 10 seconds under a voltage of 80 V.

Fig. 2. The 3mm diameter copper rode with anode status in electrolysis after 10 seconds under a voltage of 80 V.

It is observed that the copper anode has been severely corroded and has lost its effectiveness in a short time. In fact, it has been measured that more than 1 mm of the rode diameter is vanished under the oxidization process.

On the other hand, by repeating the same experiment for the gold electrodes, it has been observed that no measurable oxidization occurs on the gold electrodes. The golden anode and cathode, as shown in Fig. 3, are identical after 30s under 120V.

In order to investigate the effect of electrolysis on the produced current for each voltage, the diagram of electrical current versus voltage measured in the

presence of electrolysis along with the current-voltage diagram for the ideal case (where no electrolysis occurs) in salt water, is shown in Fig. 4.

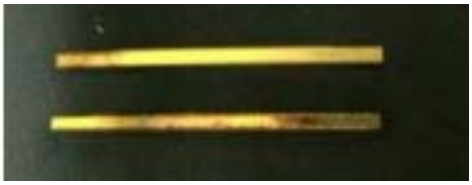

Fig. 3. Gold electrodes status in electrolysis after 10 seconds under a voltage of 120 V.

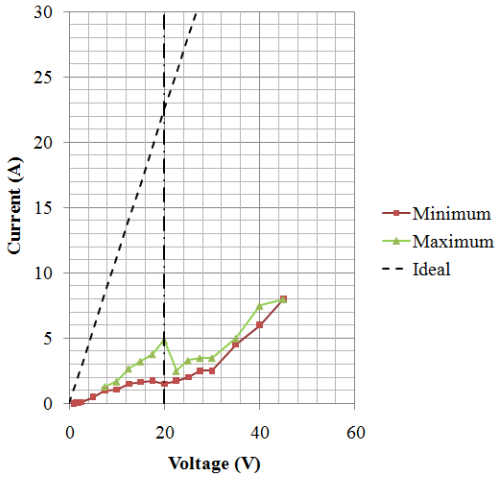

Fig. 4. Current Versus Voltage in the electrolysis test compared to the ideal case.

In order to obtain the ideal case in Fig. 4, the water conductivity of 5 S/m has been taken into account and the formula $V=IR$ has been used to calculate the expected values of the current and voltage.

In Fig. 4, the maximum and minimum values of the generated electrical current are recorded during the test. In this way, the current is recorded at the first moment as the maximum value of the current, and subsequently within 10 seconds, the minimum current occurring in the fluctuations of the current, is recorded as the minimum value of the current.

On the other hand, for the ideal case, if the water electrical resistance is considered as constant with respect to the distance between the electrodes, a resistance of 0.89 Ohm between the two electrodes is generated. The ideal state diagram, as shown in Fig. 4, represents the ideal current which should be produced at each voltage, if no electrolysis occurs and ideal conditions are assumed.

It can be seen in Fig. 4 that the difference between the experiment and the ideal state at low voltages is significant. Up to a voltage of 20 V, the distance between the maximum and the minimum current increases. This reflects the notion that electrolysis restricts a portion of the created current. However, after passing through the voltage of 20 V, the maximum and minimum values are approximately the same and change with the same trend. This is attributed to the fact that the difference in potential above 20 V takes a very short time to develop the electrolysis. Therefore, the current of the first moment has a very short life and could not be recorded by the ampere meter.

On the other hand, close scrutiny of the 10-fold difference of the ideal mode with test results, indicates that electrolysis decreases by about ten times of the current production (by reducing the exposed wetted surface of the electrodes).

Meanwhile, through increasing the voltage up to 80 volts for the copper electrode and 105 volts for the gold electrode during the test, the plasma effects are observed in the cathode, which are shown in Figs. 5 and 6, respectively. Based on these figures, it can be concluded that plasma can be obtained using gold and copper electrodes in the cathode. However, according to the results of the previous test, the copper electrodes are severely corroded at high voltages and is unusable after a short time, but the gold electrodes will never be virtually oxidized.

Fig. 5. Plasma in the cathode for copper electrodes.

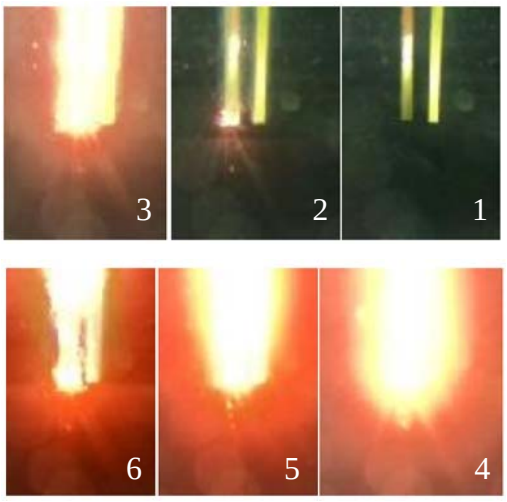

Fig. 6. Plasma in the cathode for gold electrodes.

The experiments on the magneto-hydrodynamic blanket were carried out in a pond of 1.5 meter long, 1 meter wide and 40 cm height. In order to measure the propulsion thrust force, a digital force gauge with 0.01 g accuracy, mounted on a holder above the water, was used in a way that the horizontal force of the system is applied through a lever (Fig. 7). In order to measure the accuracy of the system, a standard weight of 2 grams has been applied 30 times to the measurement system and an accuracy of 0.0012 g has been achieved.

Fig. 7. Measurement setup on the pond.

The shape and type of the magnet as well as the voltage and dimensions of the electrodes are selected based on the optimal values obtained in the previous numerical parametric investigations (Feizi and Ghadimi 2016). In that study, extensive parametric studies were carried out on a low-profile propulsive MHD blanket, and as a result, nine different parameters affecting the electromagnetic thrust and heat transfer were numerically studied. Out of 4096 items of parameters levels, 16 items were selected as samples and the optimum parameters were obtained using the Taguchi method. The illustration of the proposed optimized blanket layout is shown in Fig. 8. It should be noted that due to the limitations in the building process, the experimental setup does not fully comply with the proposed parameters in numerical analysis, but are very close.

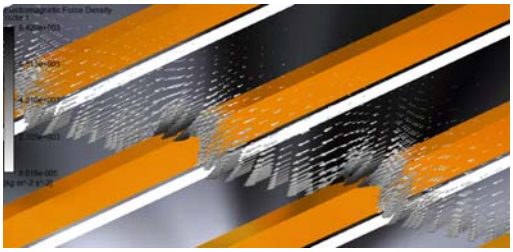

Magneto-hydrodynamic force density

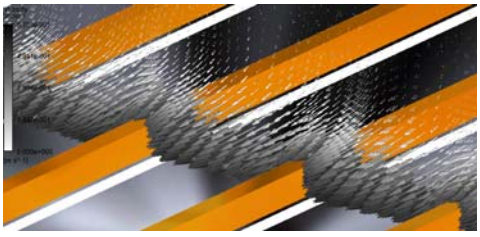

Water Velocity field

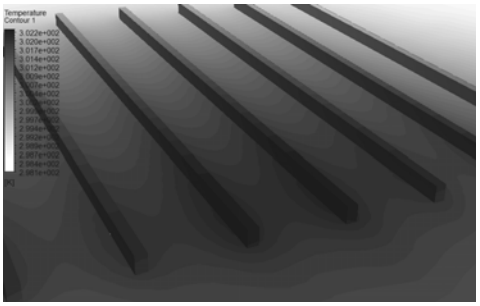

Blanket Temperature

Fig. 8. Optimized MHD blanket propulsion system from numerical analysis (Feizi and Ghadimi 2016).

The numerical analysis shown in Fig. 9 has been performed using ANSYS-CFX, which is a finite-volume based commercial code, through simultaneously modeling the fluid flow and the electric field, magnetic field, and heat transfer in the water, the solid electrodes, and electrode supports. For more details on the numerical analysis, one may refer to the previous publications of the present authors (Feizi and Ghadimi 2016).

In the next section, the results obtained from the experiments of the blankets are presented.

3. RESULTS AND DISCUSSION

Through installing a flexible magneto-hydrodynamic blanket propulsion system on a device mounted on the pond, the blankets are exposed to different voltages. In Fig. 8, the flow of water can be seen behind the blanket due to the electrolysis bubbles (the red circle at the end of the blanket). As evident in this figure, the electrolysis of water causes the production of bubbles in the system and these bubbles exit from the right side of the image with the generated flow.

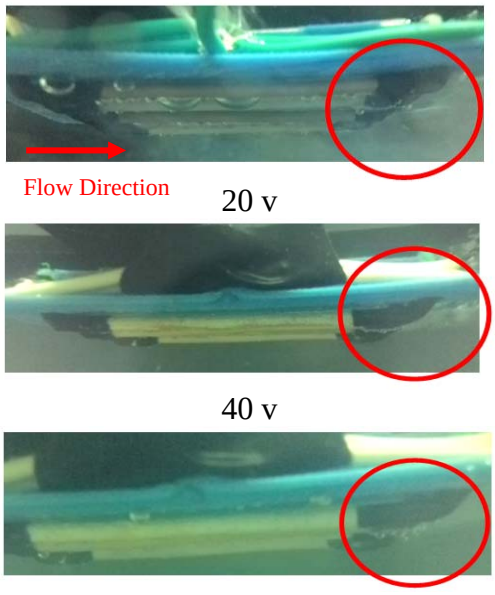

Fig. 9. Test images of the blanket in a pond at different voltages.

The MHD force generated by the blanket is measured at different voltages, and are presented in Fig. 10.

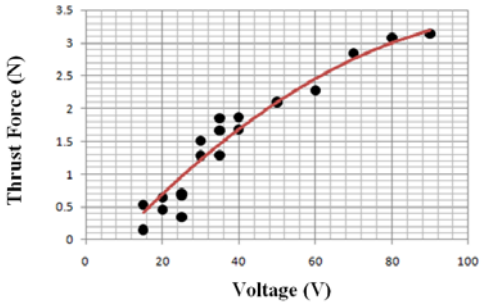

Fig. 10. System thrust force diagram at various voltages.

Each point in Fig. 10 represents a particular experiment. At some voltages, the testing is repeated several times to ensure the accuracy of the results. As observed in this figure, the results at each voltage vary by about 1mN. These changes are due to the electrolysis bubbles, since these bubbles reduce the effective area of the electrodes, and on the other hand, they are created irregularly on the electrodes and are detached from them. This causes the amount of electrical current in the water, not to be accurately predicted, but its range can be predicted.

Numerical analyses were performed on the optimal mode at 24 volts. The results of the current numerical analysis can be compared with the experimental measurements. Three tests were carried out at this voltage. Figure 11 shows a comparison of the numerical analysis (Feizi and Ghadimi 2016) and the current experimental data.

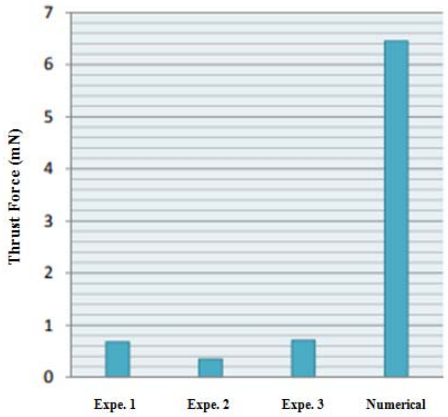

Fig. 11. Comparison of the thrust force obtained in the test and numerical analysis (Feizi and Ghadimi 2016) at a voltage of 24 V.

As evident in this figure, the obtained experimental results are between 0.37 and 0.71 mN, while the result of the numerical analysis is 45.6 mN, indicating a difference of approximately 10-fold. Due to the fact that in the numerical validation, it is demonstrated that the analysis error is 0.16%, a logical reason should be sought, apart from the numerical error for this difference. One of the most important reasons for this, which also causes the measurements to fluctuate in the conducted tests, is the electrolysis. In the numerical analysis, electrolysis was not modeled. Due to the fact that electrolysis causes the electrodes to be partly insulated, it reduces the contact surface of the electrodes with water. This leads to a decrease in the electric current in the water and finally reduces the amount of power generated by the system.

The comparison of the ideal current (without the electrolysis) and experimental current (with the electrolysis) in Fig. 4 showed a difference of ten-fold in the produced current, which justifies the difference of about 10 times difference of the experiments with the numerical analysis (without the electrolysis modeling).

Afterward, the blanket with gold anode and copper cathode with gold plating were exposed to high voltages in order to study the effect of plasma formation on the performance of the blanket.

The images obtained from applying different voltages to this blanket are shown in Fig. 12. It can be observed that at above 150 volts, the plasma is formed on the surface.

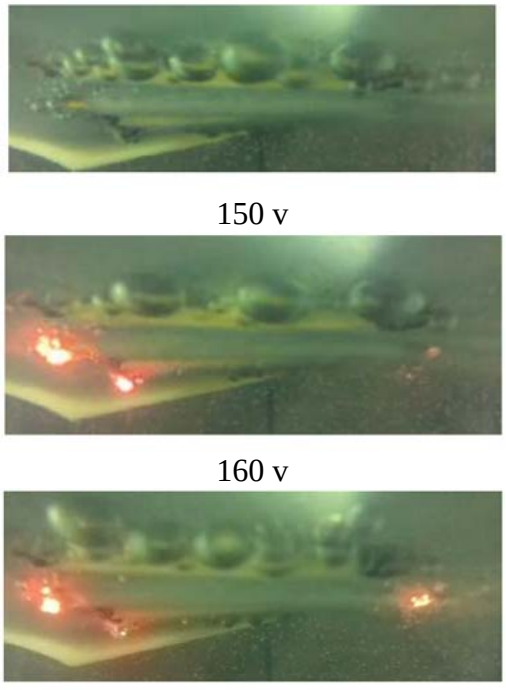

Fig. 12. Images of system performance at different voltages.

The thrust force for each voltage of this system is presented in Fig. 13.

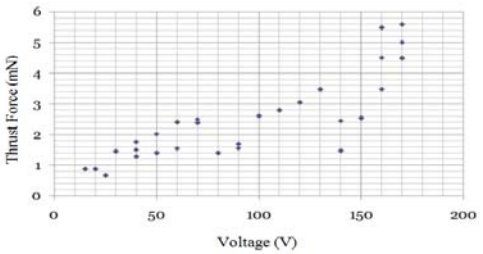

Fig. 13. Blanket force diagram versus voltage.

Due to fluctuations in the force and current, several tests have been conducted for each voltage, and the maximum and minimum force at each voltage is obtained. The important point in this diagram is that at low voltages, the behavior of the diagram is similar to that of the blanket with copper electrodes.

As evident in Fig. 13, the magnitude of this process does continue with the same trend, as expected, and at higher voltages, above 150, an impressive increase in the thrust is observed. In fact, the diagram of the system's thrust force should be broken down into three sections.

Figure 13 shows that under 130 V, due to the increase in gas volumes and electrolysis, the force variation has a certain trend. This range up to 130 volts, might be named the electrolysis range. Subsequently, the force decreases sharply in the range of 130V to 150V. This range may be called the transition range. Finally, after 160 volts, there is a sharp increase in the system's generated force, which can be called the range of thermal plasma.

As stated in the description of Fig. 12, at a voltage greater than 160 volts, the plasma effects can be observed on the blanket.

Here, it is reminded that the plasma is a state of matter in which electrons are released from the atoms and can move freely between them. Therefore, plasma is mostly considered as an electrical conductor. Therefore, if created, it should be expected to increase the electric current under a constant voltage. As the electrical current increases, the MHD force subsequently increases, as well. Therefore, the generated force, displayed in Fig. 13, greatly increases as a result of the generation of plasma and the increase in the electric current in the water.

However, the question that can be posed is why is there a significant drop in the generated force in the transitional period before the plasma is built up? The answer to this question lies in another question: Is it water or hydrogen which is producing the plasma? The fact is that the generation of plasma by the difference in the electrical potential requires that the material between the two electrodes be a dielectric type and does not conduct electricity.

In this case, it is possible that the electrons are separated from the atom by the extreme potential difference and strongly collide with other atoms and release other electrons, which in turn repeat the same process. This phenomenon is called the avalanche phenomenon and is generated in the dielectric material from the cathode to the anode. Salty water, even with low conductivity, conducts electricity and prevents the avalanch process from occurring. When the voltage increases, the electrolysis intensifies, and all paths from the cathode to the anode are blocked by the hydrogen around the cathode. More obstruction leads to further decrease in electrical current and, consequently, a decrease in MHD forces, as long as this path is completely blocked and the electric current is cut off. At this moment, due to the very high potential difference between the electrodes, the material between the cathode and the water, which is hydogen and also dielectric, reaches the point of electrical breakdown, and the avalanche phenomenon occurs and therefore, higher electrical currents occur.

For this reason, there is a significant drop in the force in the transition range since in this range, hydrogen around the cathode masks the electrode, and as soon as hydrogen atoms break down, the plasma regime begins. Off course, in this process, because of the extreme heat generated by the high water resistance, it is likely that the evaporation of water occurs and the water vapor itself acts as a dielectric gas and amplifies that process.

4. CONCLUSION

The present manuscript presents the experimental setup and the results obtained for an MHD blanket built with respect to the optimal design presented earlier by the authors (Feizi and Ghadimi, 2016) in two layouts with 3d printed support, silicon sheet support, and also copper and gold electrodes.

Although the numerical methods help investigating a wide range of parameters, the experimental study can clarify the effect of the idealizations applied in the numerical methods. It was first observed that the electrolysis decreases the electrical current production by almost 10 times with random variations. Subsequently, it has been shown that these variations, due to the electrolysis, directly affect the MHD force produced and the numerical results (where electrolysis were not modeled) are almost 10 times higher than the experiments.

To this end, after showing the difference between the gold and copper as electrodes, the possibility of plasma generation were assessed. It has been observed that, through increasing the voltage up to 80 volts for the copper electrode and 105 volts for the gold electrode, plasma effects are evident in the cathode.

Afterward, by testing the gold electrodes up to 170V, it has been demonstrated that the behavior of the propulsion produced by the blanket may be described in three regimes; the electrolysis range in which the electrolysis partly covers the electrodes and negatively affects the electric current, the transition range where the electrolysis almost completely cover the electrodes and a minimum of electric current is generated, and the plasma range where plasma is produced due to the breakdown of hydrogen gas around the cathode and a higher current is produced, highly increasing the MHD propulsion produced. Therefore, one may conclude that the main contribution of the present manuscript is the fact that it has furnished strong evidence about the possibility of increasing the MHD blanket performance through plasma production in water.

REFERENCES

Abdollahzadeh M. Y. (2014), Analytical study of

magnetohydrodynamic propulsion stability. *Journal of Marine Science and Application*, 13:281-290.

Alfve´n H. (1942) On the cosmogony of the solar system III. *Stockholms Observatoriums Ann*; 14: 9.1–9.29.

Dhanai, R., Rana, P., & Kumar, L. (2015). Multiple solutions of MHD boundary layer flow and heat transfer behavior of nanofluids induced by a power-law stretching/shrinking permeable sheet with viscous dissipation. *Powder Technology*, 273, 62-70.

Doss, E. D. and Roy, G. D. (1990, August). Three-dimensional parametric study for MHD marine propulsion. In Energy Conversion Engineering Conference, 1990. IECEC-90. *Proceedings of the 25th Intersociety* (Vol. 5, pp. 508-513). IEEE.

Feizi Chekab, M. A., & Ghadimi, P. (2017). Curvature Effects on the Electromagnetic Force, Efficiency, and Heat Transfer of a Weak Low Profile Magneto-Hydrodynamic Blanket Propulsion System. *Journal of Applied Fluid Mechanics*, 10(5), 1261-1270.

Friauf J. (1961), Electromagnetic ship propulsion, *ASNE J*, Vol. 139, p. 142.

Gilbert II J. B. and Lin T. F. (1995), Analytical and experimental studies of the helical magnetohydrodynamic thruster design. *International Journal of Offshore and Polar Engineering*, 5, 91-97.

Hales, P., Hirst, P., Milward, S., Harrison, S., & Jones, H. (2006). A solid-nitrogen cooled high-temperature superconducting magnet for use in magnetohydrodynamic marine propulsion. *IEEE transactions on applied superconductivity*, 16(2), 1419-1422. Han J., Sha C. W., Peng Y. (2002), Simulation and analysis of an alternating magnetic field MHD thruster. *INEC 2002: The Marine Engineer in the Electronic Age-Conference Proceedings*, 317-322.

Hartman, J., & Lazarus, F. (1937). Experimental investigations on the flow of mercury in a homogeneous magnetic field, *Hg-Dynamics II. Math. Fys. Med*, 15, 145.

Kantrowitz, A. R., Brogan, T. R., Rosa, R. J., & Louis, J. F. (1962). The magnetohydrodynamic power generator-basic principles, state of the art, and areas of application. *IRE Transactions on Military Electronics*, 1051(1), 78-83.

Lin T. F., Aumiller D. L., Gilbert II J. B., Cusin M. J., Brandt B.I., Rubin L.G. (1992), Study of the influence of electric and magnetic fields on seawater magnetohydrodynamic propulsion. *Proceedings of the Second International Offshore and Polar Engineering Conference*, US, 3, 8-13.

Lint, T. F., Gilbert, J. B., Naggar, J. A., & Imblum, T. M. (1991). Seawater conductivity enhancement by acid injection for the MHD thrusters. In: *Oceans conference record (IEEE)*; 3: 1629–1635.

Lin TF. (1990) Considerations of sea water conductivity enhancement for electromagnetic thrusters. In: *Proceedings of the intersociety energy conversion engineering conference* vol. 5:, pp.552–556.

Meng, J. C. S., Hrubes, J. D., Hendricks, P. J., Thivierge, D. P., & Henoch, C. W. (1991), Experimental studies of a superconducting electromagnetic thruster for seawater propulsion and future technological challenges. In: *Oceans conference record* (IEEE) 1991; 3: 1613–1620.

Motora S., Takezawa S., Tamama H. (1991) Development of the MHD ship YAMATO-1. *Oceans Conference Record (IEEE)*, 3, 1636-1641.

Popov YP. (1971), Calculation of electric circuits in magnetohydrodynamic problems. *USSR Comput Math Phys*; 11: 183–196.

Rice W. A. (1961), *Rice propulsion system*, Patent: US2997013.

Stenflo JO. (2017) History of solar magnetic fields since George Ellery Hale. S*pace Science Reviews*, 210(1-4), 5-35.

Skála, J., Baruffa, F., Büchner, J., & Rampp, M. (2015) The 3D MHD code GOEMHD3 for astrophysical plasmas with large Reynolds numbers: code description, verification, and computational performance. *Astron Astrophys*; 580(A48). Smy PR. (1961) Alternating current magnetohydrodynamic generator. *J Appl Phys*; 32: 1946–1951.

Way S. (1967), Electromagnetic propulsion for cargo submarines. *AIAA–paper*, 1967–0363.

Weier T, Shatrov V and Gerbeth G. (2007) Magnetohydrodynamics: Evolution of ideas and trends: *flow control and propulsion in poor conductors*. Netherland: Springer, pp.295–312.

Wu YK. (1973) Magnetohydrodynamic boundary layer control with suction or injection. *J Appl Phys*; 44: 2166–2171.

Yan, L., Sha, C., Peng, Y., Zhou, K., Yang, A., & Qing, Q. (2002) Results from a 14T superconducting MHD propulsion experiment. In: *33rd plasma dynamics and lasers conference*, p. 2172.

Zhang C, Xing D. and Li, Y. (2007) Micropumps, microvalves, and micromixers within PCR microfluidic chips*: advances and trends. Biotechnol Adv*; 25: 483–514.